

Electronic Supporting Information

Chelate stabilized metal oxides for visible light photocatalyzed water oxidations

*Dominic Walsh**, *Noelia M Sanchez-Ballester*, *Katsuhiko Ariga*, *Akihiro Tanaka*, *Mark Weller**

Instrumentation

TEM

Samples mounted on formvar coated copper mesh grids were examined using Jeol 1200 EXII TEM's operating at 120kV with attached gatan dual view digital camera.

Powder X-ray diffraction

Siemens D5000 powder X-ray diffractometer (CuK α)

Energy Dispersive X-ray analysis

EDX elemental analysis on the TEM was conducted using a Thermo-Fisher ultra-dry SDD EDS with Noran 7 software for quantitative analysis.

X-ray Photoelectron Spectroscopy

XPS of samples was conducted on a ULVAC-PHI Model: Quantera/SXM XPS with collection conditions as follows:

X-ray=Al monochromatic 1486.7 eV, Anode power=100W (20kV, 5mA)

Irradiation area: 1.4mm X 0.3mm, Neutralization: electron 1.4 eV (20 micro-A), Ar ion 7 eV (30 nA)

Analysis conditions

Survey spectra: Pass energy=280 eV, Energy step=0.5 eV

Multiplex: Pass energy= 55 eV, Energy step=0.1 eV

Thermogravimetric measurements

Thermogravimetric (TGA) analysis of chelated samples was conducted using a Polymer Laboratories PL-STA TGA with ISI Thermal Analysis software. Weight loss of samples heated in air at 10°C/min up to 800°C were recorded.

Surface area analysis (BET)

N₂ physisorption isotherms for surface area measurement of samples was conducted with a Micromeritics-TriStar 3000 after degassing for 3 hrs at 120°C. The surface area was calculated from the linear part of the BET plot (5 point measurement).

Dynamic Light Scattering (DLS)

0.1-0.4mg/ml solutions filtered through 0.22 μ m filters were analysed by DLS using a Malvern Zetasizer MS.

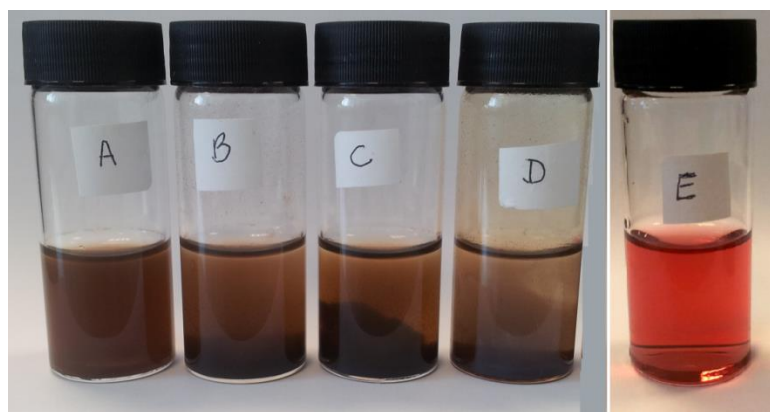
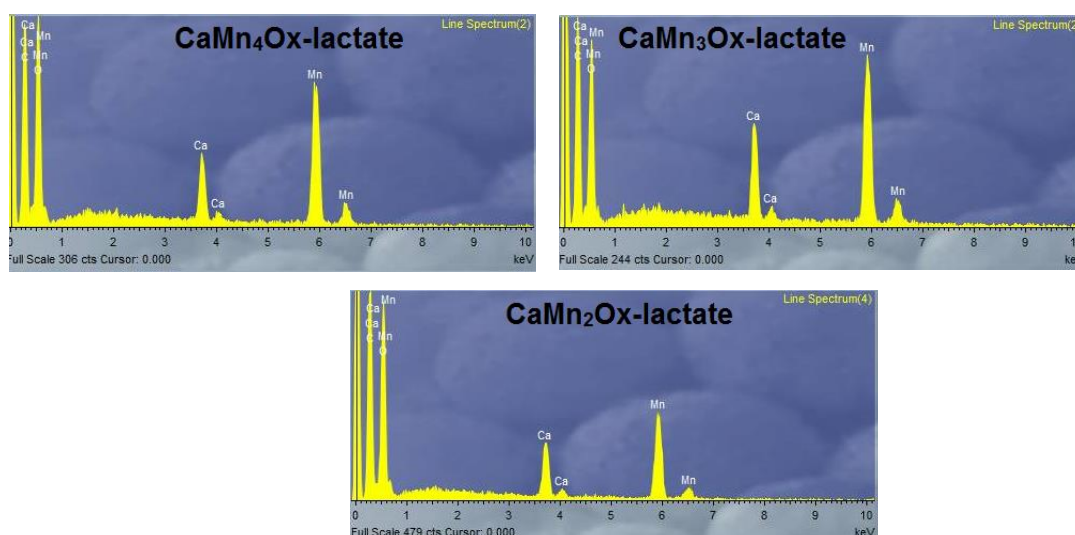


Fig. S1a. Image of aqueous solutions of (a) Mn_3O_4 -lactate; (b) CaMn_4Ox -lactate; (c) CaMn_3Ox -lactate; (d) CaMn_2Ox -lactate; (e) CoOx -lactate(1nm). (After storing under quiescent conditions for several hours).



Sample	Mean Ca:Mn molar ratio	Maximum and minimum ranges
CaMn_4Ox -lactate	1:4.12	1:3.7 – 1:4.4
CaMn_3Ox -lactate	1:3.08	1:2.8- 1:3.3
CaMn_2Ox -lactate	1:2.42	1:1.4 – 1:3.2

Fig. S1b. Representative quantitative SEM spot EDX analysis and table of prepared particles showing mean (average of 10 spots taken from differing particles of each sample) and maximum/minimum ranges of Ca:Mn molar ratios. The CaMn_2Ox -lactate sample was significantly less homogeneous compared to the other samples.

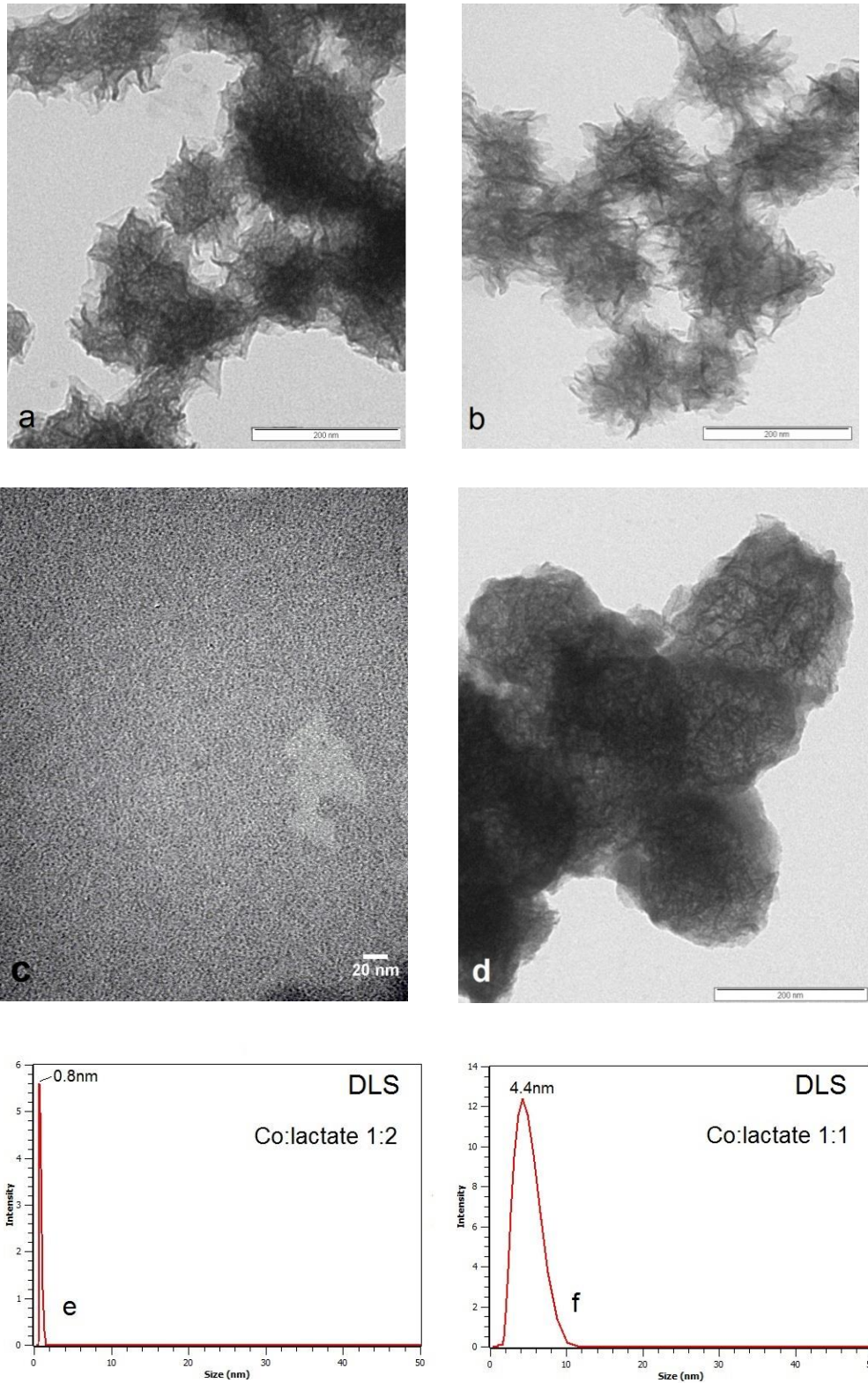


Fig. S2. TEM images showing (a) prepared CaMn_4Ox -lactate; (b) prepared CaMn_2Ox -lactate; Co:lactate 1:2 (1-2nm); (d) CaMn_3Ox -lactate spherules recovered from a 200min photocatalytic reaction showing coating of nanoparticulate cobalt oxides formed in-situ. (e) DLS of Co:lactate 1:2 with intensity centered around 0.8 nm; (f) DLS of Co:lactate 1:1 with intensity centered around 4.4nm

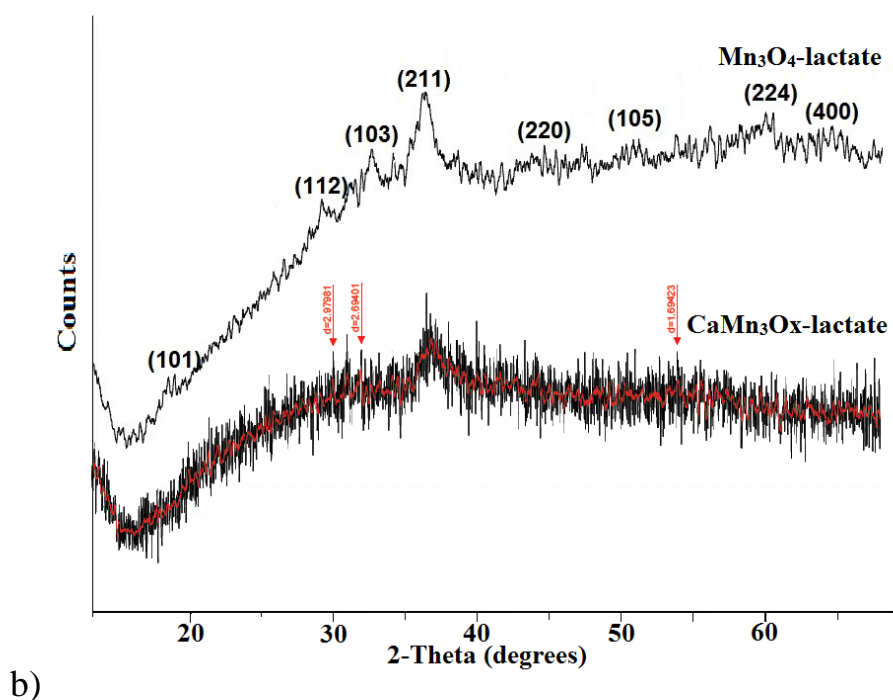
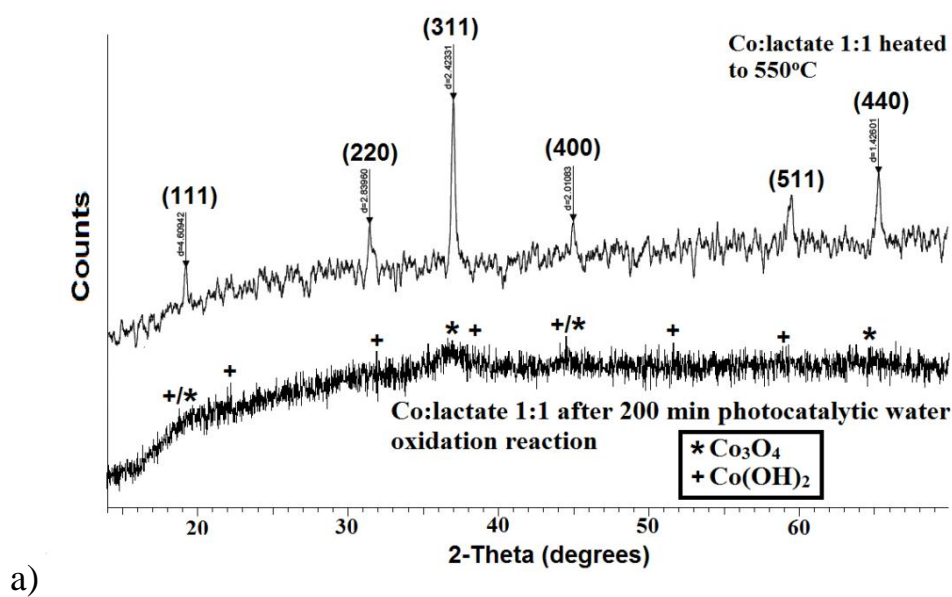


Fig. S3. Powder XRD of (a) Co:lactate 1:1 recovered from 200 min photocatalytic reaction showing reflection due to Co_3O_4 and $\text{Co}(\text{OH})_2$ and after heat treatment to 550°C for 2.5 hrs. showing reflections due to cubic Co_3O_4 (Co_3O_4 and $\text{Co}(\text{OH})_2$ ICDD patterns 00-042-1467, 00-002-0925 and ref. 1); (b) Mn_3O_4 -lactate and CaMn_3O_x -lactate heated to 325°C for 3 hrs (to minimize phase changes). Mn_3O_4 -lactate shows reflections due to tetragonal Mn_3O_4 (from ICDD pattern 00-024-0734), the diffraction pattern obtained with CaMn_3O_x -lactate is broadly similar with some possible additional reflections indicating a $\text{Ca}_x\text{Mn}_y\text{O}_z$ phase (similar to $\text{Ca}_2\text{Mn}_3\text{O}_8$ (ICDD 01-073-2290)).

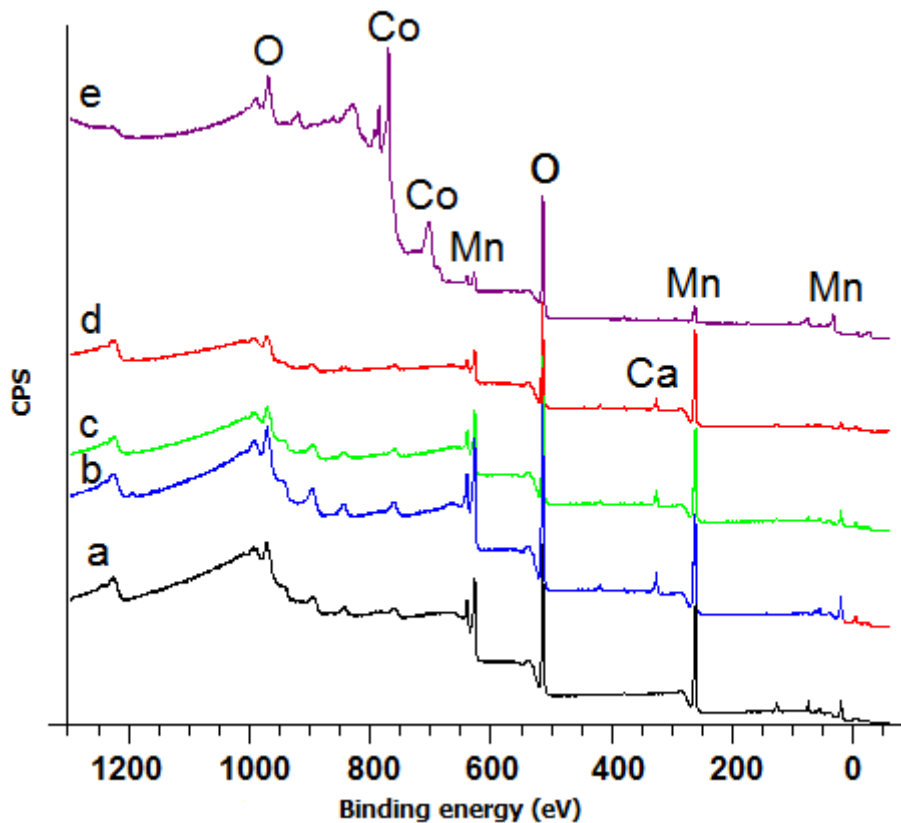


Fig. S4. XPS analysis of washed samples of (a) Mn_3O_4 -lactate; (b) CaMn_4O_x -lactate; (c) CaMn_3O_x -lactate; (d) CaMn_2O_x -lactate; (Atomic % of Ca and Mn correspond to mole ratios of Ca:Mn of 1:6.8, 1:5.3, and 1:3.3 for CaMn_4O_x -lactate, CaMn_3O_x -lactate and CaMn_2O_x -lactate respectively). (e) CaMn_3O_x -lactate catalyst recovered after use in a 200min photocatalytic water oxidation reaction. Calcium ions have been removed by dissolution and cobalt ions from the decomposed electron acceptor precipitated as oxide on the lactate substrate particles. (Atomic % of the Co and Mn correspond to a mole ratio of 7.3:1 at the surface of the lactate particles).

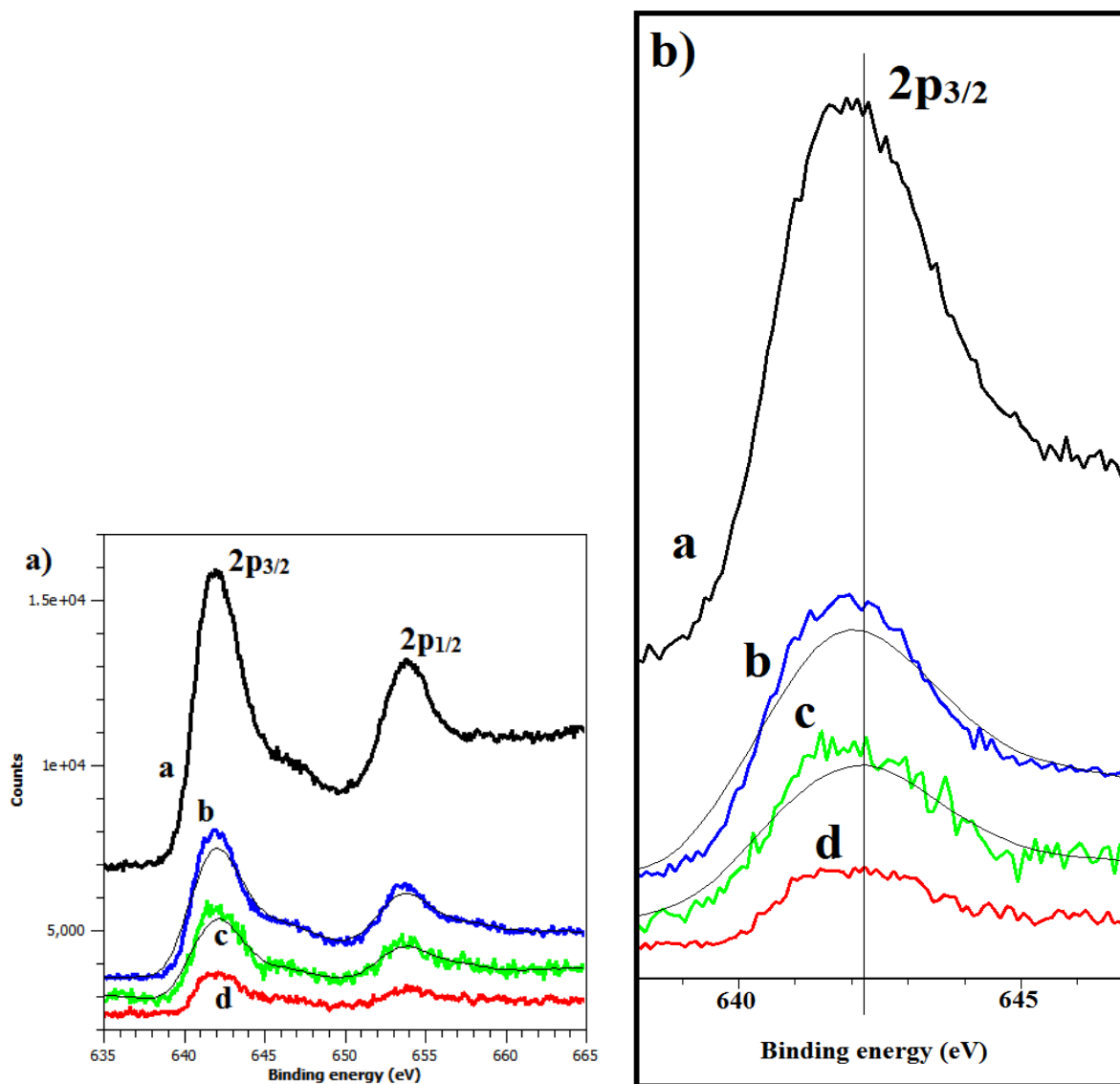


Fig. S5(a). XPS of Mn2p region showing (a) Mn₃O₄-lactate; (b) CaMn₄Ox-lactate; (c) CaMn₃Ox-lactate; (d) CaMn₂Ox-lactate. Diminishing peak sizes are due to reduced relative levels of Mn present; (b) enlargement showing small shift to higher binding energy of the CaMn₃Ox-lactate 2p_{3/2} band.

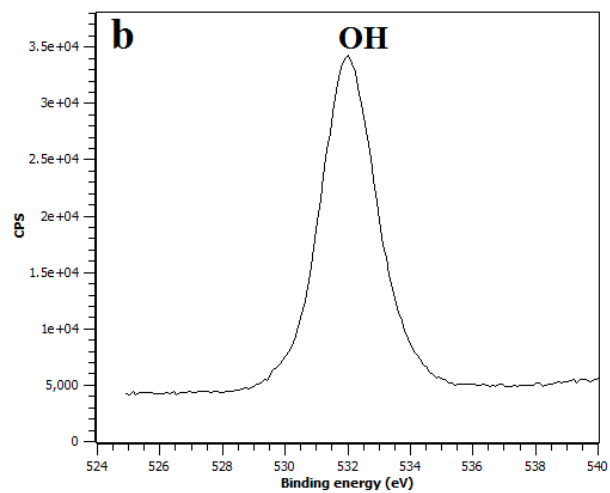
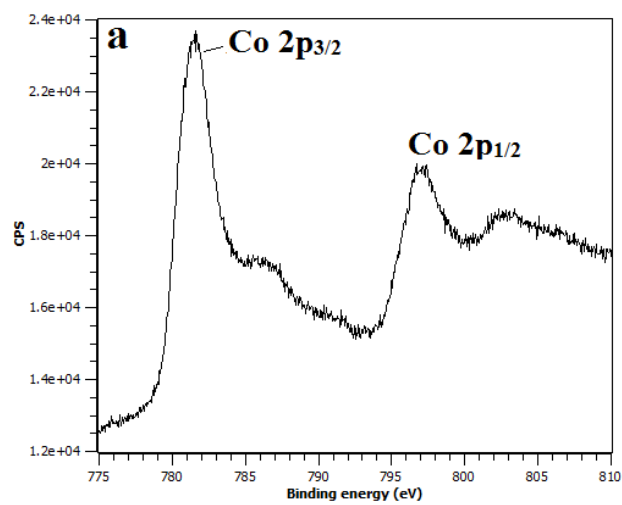


Fig. S6. XPS analysis of Co:lactate 1:2 showing (a) 2p region showing peaks corresponding in position and shape to Co^{2+} bound to hydroxyls.(b) O 1s region showing peak due to hydroxyl groups at 532eV.^{2,3}

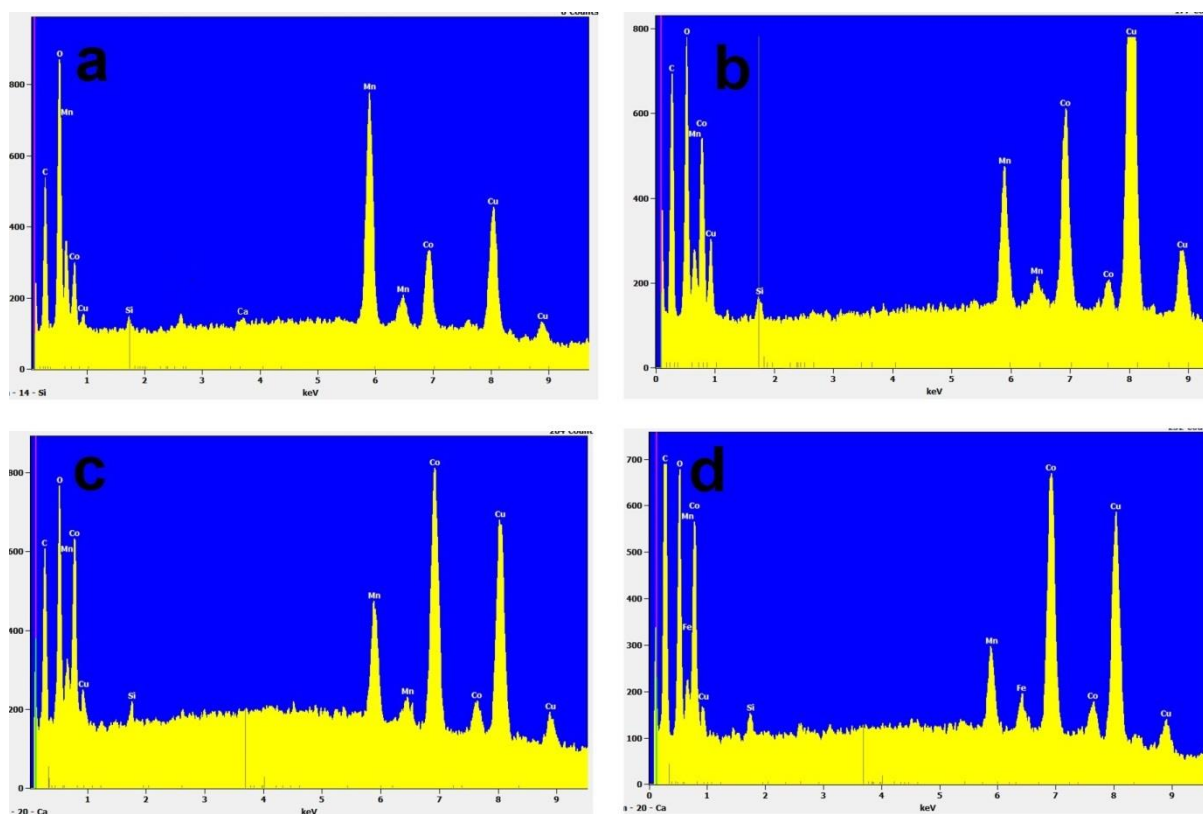


Fig. S7. EDX analysis of CaMn_3O_x -lactate samples collected from a photocatalytic reaction after (a) 50min; (b) 100min; (c) 150 min; (d) 200 min. Showing increase in level of bound cobalt with increasing reaction time. (Triplicate measurements were taken which were consistent, representative spectra are shown).

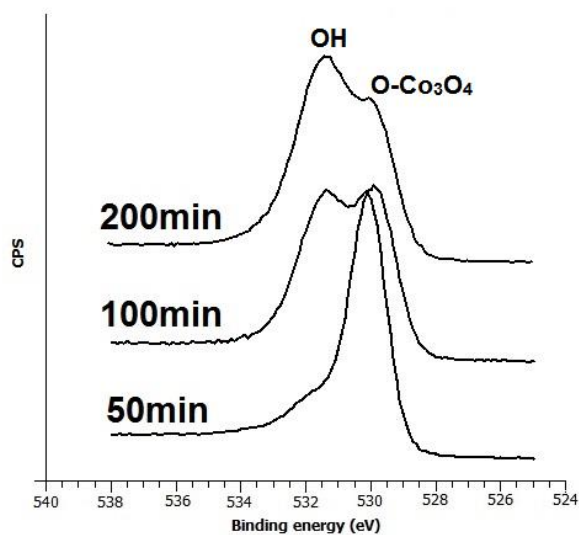


Fig. S8. High resolution XPS analysis of CaMn_3O_x -lactate catalysed photocatalytic reaction with washed samples recovered at intervals showing the O 1s region showing peak due to Co_3O_4 lattice O^{2-} at 530eV, and peaks due to hydroxyls at 531.4 that increase in intensity with increasing reaction time.^{2,3}

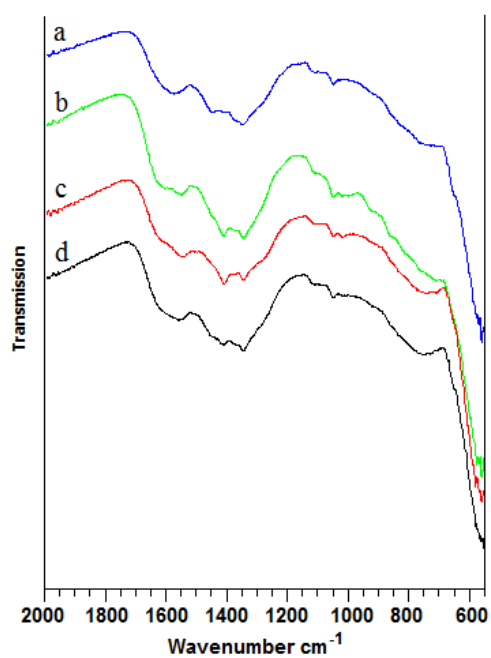


Fig. S9. FT-IR of calcium-manganese-oxide lactate samples recovered after a photocatalytic water reaction showing (a) CaMn₂O_x-lactate; (b) CaMn₃O_x-lactate; (c) CaMn₄O_x-lactate; (d) Mn₃O₄-lactate. Absorption bands due to lactate (CO₂⁻) are present in all samples.

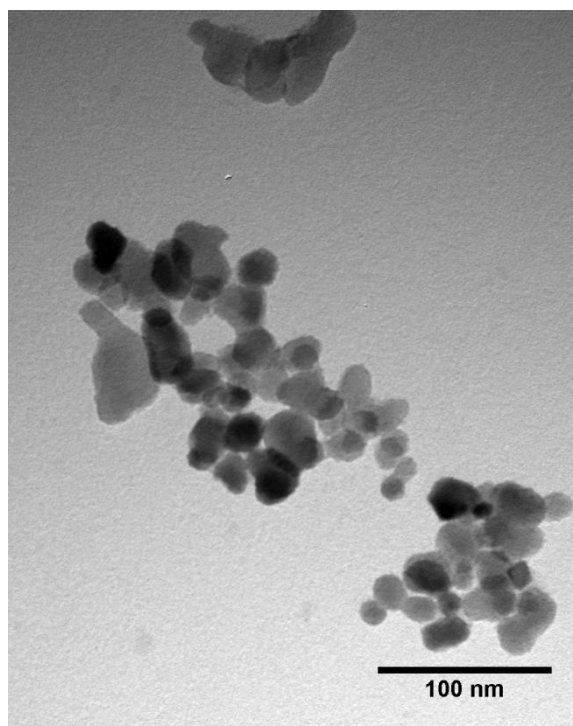


Fig. S10. TEM image of commercial laser ablated Co_3O_4 catalyst nanoparticles recovered from photocatalytic reaction after 200 min, showing negligible accumulation of cobalt material from decomposed electron acceptor.

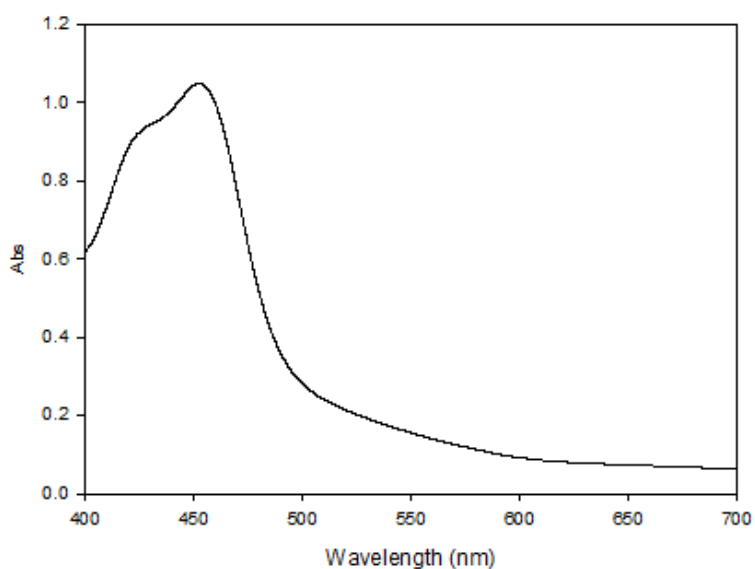


Fig. S11. Visible light absorption spectrum of a $\text{CaMn}_3\text{Ox-lactate-}[\text{Ru}(\text{bipy})_3]\text{Cl}_2\text{-}[\text{Co}(\text{NH}_3)\text{Cl}]\text{Cl}_2$ photocatalytic reaction mixture showing absorption maximum at 453nm.

Example of Turn over Frequency calculation

Taking as example the commercial Co₃O₄ nanopowder

10mg of Co₃O₄ = 7.342mg of Co present in photocatalytic reaction

Moles = 7.342mg/58.93 = 0.1245 x 10⁻³ moles

Measured maximum level of O₂ generation was 0.033μmol per second

TOF = 0.033μmol / 0.1245 x 10⁻³ moles s = 0.2651 x 10⁻³ mol (O₂)/ mol (Co) s)

TOF = 0.265 x 10⁻³ mol (O₂)/ mol (Co) s) (at the initial linear O₂ generation period)

TOF's for other catalysts were determined similarly and were normalized to active metal content (i.e. taking into account the reduced levels of the active Mn component present with the calcium containing bimetallic oxides).

Example of Quantum Yield (Φ) calculation

Since the results showed that surface areas of the catalysts changed continuously throughout the reaction a photonic method was used for determining Quantum Yields.

Taking as example the commercial Co₃O₄ nanopowder

Using wavelength of 452nm, intensity of light measured at 1.3mW/cm² impinging on 30.8cm² surface = 40mW, time to maximum O₂ yield = 80 min.

Energy of a single photon at 452nm = h.c/λ

= 6.626x10⁻³⁴ x 2.998 x 10⁸/ 452 x 10⁻⁹ = 4.365 x 10⁻¹⁹ J

Total power absorbed = 40mW x 80 min x 60 = 192 J

Number of O₂ molecules produced = 71μmol x 6.022 x 10²³ = 4.276 x 10¹⁹

Taking that 4 photons are absorbed per O₂

Quantum Yield Φ = 4.276 x 10¹⁹ / (192 J/ 4.365 x 10⁻¹⁹ J) x 400% = 38.9%

Φ with other catalysts were calculated similarly taking into consideration time to maximum O₂ yields.

References

1. P. Jeevanandam, Yu. Kolytyn, A. Gedanken and Y. Mastai, *Journal of Materials Chemistry*, 2000, 10, 511-514.
2. S. C. Petitto and M. A. Langell, *Journal of Vacuum Science & Technology A*, 2004, 22, 1690-1696.
3. W. Guo, Y. E, I. Gao, L. Fan and S. Yang, *Chemical Communications*, 2010, 46, 1290-1292.